

ORIGINAL PAPER

Combustion-derived CdO nanopowder as a heterogeneous basic catalyst for efficient synthesis of sulfonamides from aromatic amines using *p*-toluenesulfonyl chloride

^aBelladamadu Siddappa Anandakumar, ^aMuthukur Bhojgowd Madhusudana Reddy, ^bKumarappa Veerappa Thipperudraiah, ^aMohamed Afzal Pasha, ^aGujjarahalli Thimmanna Chandrappa*

^aDepartment of Chemistry, Bangalore University, Bangalore-560001, India

^bDepartment of Physics, National Degree College, Jayanagar, Bangalore-560070, India

Received 1 December 2011; Revised 1 May 2012; Accepted 14 May 2012

A simple and rapid synthesis of CdO nanopowder via the solution combustion route employing L-(+)-tartaric acid as a fuel is reported for the first time. The catalyst was characterized by PXRD, SEM, TEM, BET surface area measurement, basic site measurement from back titration and FTIR. Combustion derived CdO nanopowder acts as a catalyst in the sulfonylation of amines with *p*-toluenesulfonyl chloride to obtain sulfonamides in excellent yield (85–95 %) and high purity under mild reaction conditions. CdO nanopowder has been found to be an efficient catalyst requiring a shorter reaction time (10–30 min) to obtain sulfonamide when compared with the commercial CdO powder requiring 2 h under similar conditions. The catalyst can be recovered and reused four times without any significant loss of catalytic activity. Potential role of CdO nanopowder in the synthesis of sulfonamides and its mechanism is proposed.

© 2012 Institute of Chemistry, Slovak Academy of Sciences

Keywords: nanopowder, solution combustion, amines, *p*-toluenesulfonyl chloride, tartaric acid, sulfonamide

Introduction

Transition metal oxides of nanometric size have attracted considerable attention because of their unique properties and potential for extensive applications in catalysis, electronics, and environment. Recently, several transition metal oxides (Thakuria et al., 2007; Gliński et al., 1995) including CdO (Mazaheritehrani et al., 2010; Alves et al., 2010; Abd El-Salaam & Hassan, 1982; Okuhara & Tanaka, 1980; Balandin et al., 1960) have been used as catalysts in organic synthesis because of their beneficial physicochemical properties such as particle size, large surface area and tunable pore structure. In addition to the large surface area, their strong basic active sites make CdO nanopowder a promising catalyst in organic synthesis. It is

also widely used for gas sensors, solar cells, and optics as well as in catalysis. Over the past two decades, several methods such as sol-gel (Santos-Cruz et al., 2007; Ashoka et al., 2010), sonochemical, and coprecipitation methods (Askarinejad & Morsali, 2008; Waghulade, et al., 2007) have been developed for the synthesis of CdO nanopowder. Solution combustion synthesis (Patil et al., 2008; Nagappa & Chandrappa, 2007) is one of the most fruitful methods for the synthesis of metal oxide nanoparticles in general and CdO nanopowder in particular because of its shorter reaction time at ambient conditions and its low cost with a potential to scale up. In addition, this method is useful for the production of homogeneous, porous, and fine crystalline powders. To the best of our knowledge, the synthesis of CdO nanopowder via the solution com-

*Corresponding author, e-mail: gtchandrappa@yahoo.co.in

bustion method has not been reported so far.

In the present investigation, tartaric acid was used as the fuel in the synthesis of CdO nanopowder via a solution combustion route. Combustion derived CdO nanopowder possesses a large surface area with large porosity. The large surface area can provide a greater number of active sites than the low coordinated oxide sites (edges, corners) (Sterrer et al., 2003) and lattice defects (cation and anion vacancies) (Sousa et al., 1999). The pore diameter of CdO nanopowder is another key factor affecting the contact performance between the reactant and the catalyst (Znahg et al., 2009). Higher surface area of the nano powder can provide more active sites, whereas a porous structure facilitates the adsorption and diffusion of reactant molecules. Both factors enhance the catalytic performance in the present system (Davis, 2002). In addition, the CdO nanopowder possesses a greater number of basic sites as compared to commercial CdO. Therefore, CdO nanopowder can act as a strong Lewis base in catalytic reactions. It has been found that heterogeneous basic catalysts have more advantages over the homogeneous organic basic catalysts, e.g. easy recovery of the catalyst, simple isolation, recyclability, and minimization of metal oxide impurities in the product. Thus, heterogeneous basic catalysts have been recognized as a potential alternative to the homogeneous organic basic catalysts.

Sulfonylation of amines is an important step in synthetic organic chemistry. The sulfonyl group is one of the most versatile amino- or hydroxyl-protecting groups in organic synthesis (Nishida et al., 1988; Yuan et al., 1989; O'Connell & Rapoport, 1992; Chandrasekhar & Mahapatra, 1998). Sulfonyl derivatives are useful as drugs and they exhibit a wide-range of biological activities such as anti-cancer, anti-inflammatory, and anti-viral functions (Supuran et al., 2003; Scozzafava et al., 2003; Harter et al., 2004; Reddy et al., 2004; Stranix et al., 2006). Many of the methods (Anderson, 1979; Russell et al., 2001) reported for the synthesis of sulfonamides have limitations such as harsh reaction conditions (Poissonnet et al., 1996), long reaction time (Yasuhara et al., 1999), the use of toxic reagents such as pyridine, and difficult catalyst recovery (Chan & Berthelette, 2002). To overcome all these drawbacks, a general, mild, and novel method to synthesize sulfonamides has been developed.

Our ongoing research program is aimed at the development of a heterogeneous catalyst to synthesize widely used organic compounds (Madhusudana Reddy et al., 2010, 2011).

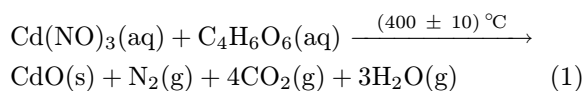
Studies on organic reactions catalyzed by CdO nanopowder are very scarce and no reports on the synthesis of sulfonamides are available. It is therefore desirable to develop a new green and reusable catalyst for this synthesis; the use of CdO nanopowder prepared via a low temperature solution combus-

tion method was investigated. Catalytic activity of the CdO nanopowder was evaluated for the sulfonylation reaction of amines with *p*-toluenesulfonyl chloride (*p*-TsCl) using acetonitrile solvent under reflux conditions. Catalytic activity of commercial CdO powder in comparison with the combustion derived CdO was also examined.

Experimental

Cadmium nitrate tetrahydrate of the purity of 99 %, L-(+)-tartaric acid crystals of the purity of 99.7 %, and commercial CdO powder of the purity of 99 % were purchased from Merck Chemicals, India. Commercial CdO powder had the particle size of 0.5–1.5 μm and the BET specific surface area of 3–4 $\text{m}^2 \text{g}^{-1}$. All organic chemicals used were commercial grade and all solid amines were used without further purification, liquid amines were distilled before use.

An aqueous solution containing cadmium nitrate as the oxidizer (O) and tartaric acid as the fuel (F) (corresponding F : O ratio $\phi = 1$ as shown in (Eq. (1))) was put in a pyrex dish (Nagappa & Chandrappa, 2007). Excess water was evaporated by heating on a hot plate until a viscous gel was formed. The pyrex dish was then placed in a muffle furnace maintained at $(400 \pm 10)^\circ\text{C}$. Initially, the reaction mixture underwent dehydration followed by smoldering (low flame) combustion. The product, cadmium oxide nanopowder, left behind was porous and voluminous.



In the general procedure for sulfonylation of aromatic amines, *p*-toluenesulfonyl chloride (5.5 mmol) and CdO nanopowder (1 mole %) were added to a solution of aromatic amines (5 mmol) in acetonitrile (5 mL). The reaction mixture was stirred at reflux for 10–30 min (Fig. 1). The progress of the reaction was monitored by thin-layer chromatography (TLC) and after its completion, the reaction mixture was cooled to room temperature (r.t.), the CdO nanopowder suspension was filtered using a cellulose nitrate membrane filter Whatman (Scientific & Surgical Corporations, India) and extracted with ethylacetate (20 mL). Organic extract was dried using anhydrous MgSO_4 and concentrated under reduced pressure. In all cases, products obtained from the sulfonamides were pure.

Powder X-ray diffraction patterns were obtained by a Philips X'pert PRO X-ray diffractometer (PANalytical, B. V. Almelo, Netherlands SPECTRIS PTE, The Netherland) using $\text{CuK}\alpha$ radiation ($\lambda = 1.54056 \text{ \AA}$) at the scanning rate of 0.02° per second for 2θ in the range from 10° to 70° and operated at 40 kV and 30 mA. Morphologies of the products were examined by a Quanta-200 scanning electron microscope (JEOL, Japan) equipped with an energy dis-

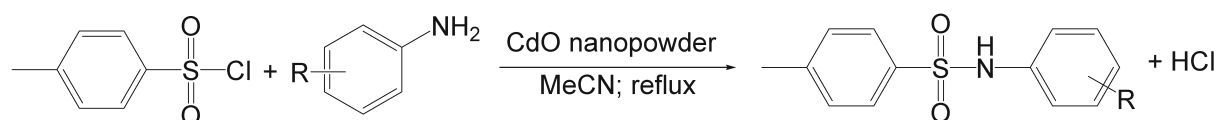


Fig. 1. Scheme of general procedure for sulfonylation of aromatic amines with *p*-TsCl and CdO nanopowder. R = CH₃, F, Cl, Br, OCH₃, NO₂.

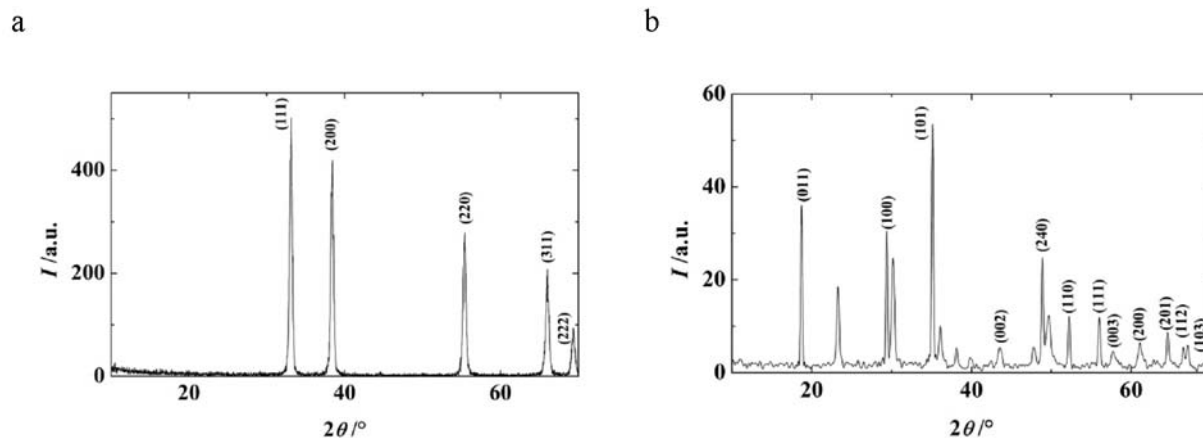


Fig. 2. PXRD pattern of CdO nanopowder (a) and H⁺ ion adsorbed on the CdO nanopowder (b).

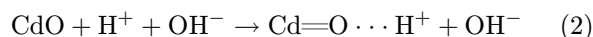
persive X-ray spectroscopy (JEOL, Japan). Samples were gold-coated prior to the scanning electron microscopy (SEM) analysis. Nano/microstructure of the products was observed by transmission electron microscopy (TEM) and selected-area electron diffraction (SAED) which was performed with a Hitachi model H-600 instrument (White Brook Park, UK) operating at 100 kV. Surface area measurements and pore size distribution analysis were done after degassing the sample under high vacuum at 300 °C for 4 h; and nitrogen adsorption measurements were carried out at 77 K using a gas sorption analyzer Quanta chrome corporation NOVA 1000 (Quantachrome Instruments, USA). All melting points were determined using a Büchi apparatus. Nuclear magnetic resonance spectra were obtained on a 400 MHz Bruker AMX spectrometer (IET, USA) in DMSO-*d*₆ using TMS as the standard. GC-mass spectra were obtained using a Shimadzu GC-MS QP 5050A instrument (SpectraLab Scientific, Canada) equipped with a 30 m long BP-5 column with the diameter of 0.32 mm and the column temperature of 80–15–250 °C. Infrared spectra were recorded using a Shimadzu FT-IR-8400s spectrometer (Shimadzu Corporation, Japan) as KBr pellets for solids and as thin films between NaCl plates for liquids.

Results and discussion

Powder X-ray diffraction

Powder X-ray diffraction patterns were obtained on a Philips X'pert PRO X-ray diffractometer using

CuK_α radiation. The PXRD pattern clearly shows that CdO crystalline powder is in the cubic phase with lattice constant $a = 4.695 \text{ \AA}$ (JCPDS 75-0594) as shown in Fig. 1a. Broadness of the peaks indicates the nanocrystalline nature of the CdO nanopowder and the particle size calculated from the Scherrer's formula is in the range of 40–60 nm. The amount of basic sites present in the CdO nanopowder was determined by back titration. Eq. (2) presents the proposed mechanism of the determination of the amount of basic sites.



In this reaction, the prepared CdO nanopowder was allowed to stand in distilled water for 24 h to let the nanoparticles of CdO submerge into distilled water. The H⁺ ion was provided by distilled water, it was absorbed by the lone pair of oxygen from the CdO nanopowder and the OH⁻ ion was formed. This technique helps to estimate the amount of H⁺ ions absorbed by the prepared CdO nanopowder. Finally, the H⁺ ions formed a bond with the CdO nanopowder resulting in the formation of Cd(OH)₂. The H⁺ ion adsorbed on the CdO nanopowder is shown in the PXRD pattern in Fig. 2b. All diffraction peaks can be indexed to hexagonal crystal structure of Cd(OH)₂ which is in good agreement with the reported data and with the respective JCPDF card no 73-0969.

The formation of Cd(OH)₂ can be caused by the reaction between the CdO nanopowder with water (Nondek et al., 1979; Samadi et al., 2010).

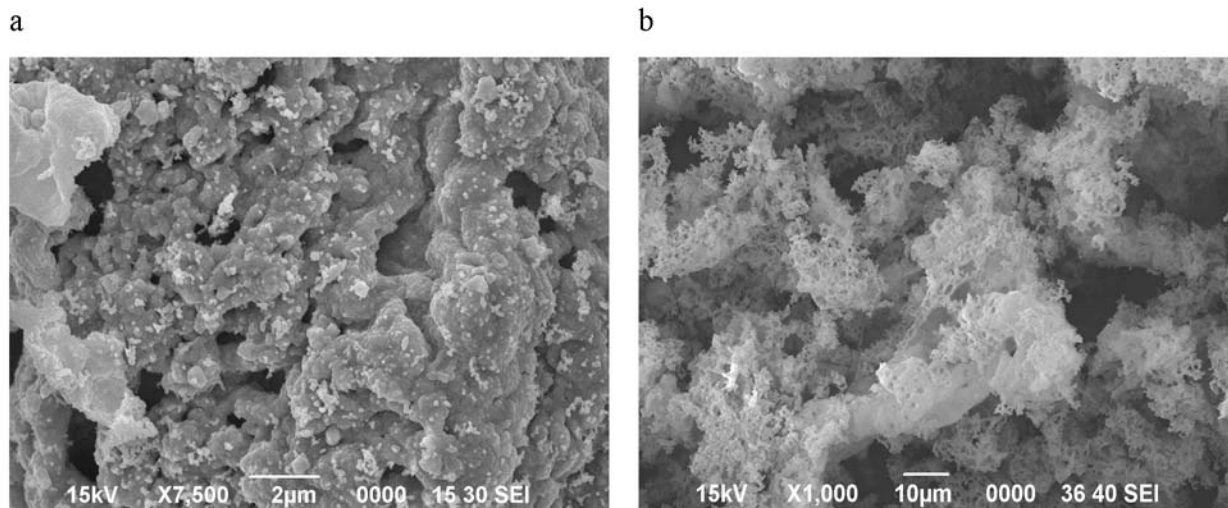


Fig. 3. SEM image of commercial CdO powder (a) and SEM image of CdO nanopowder (b).

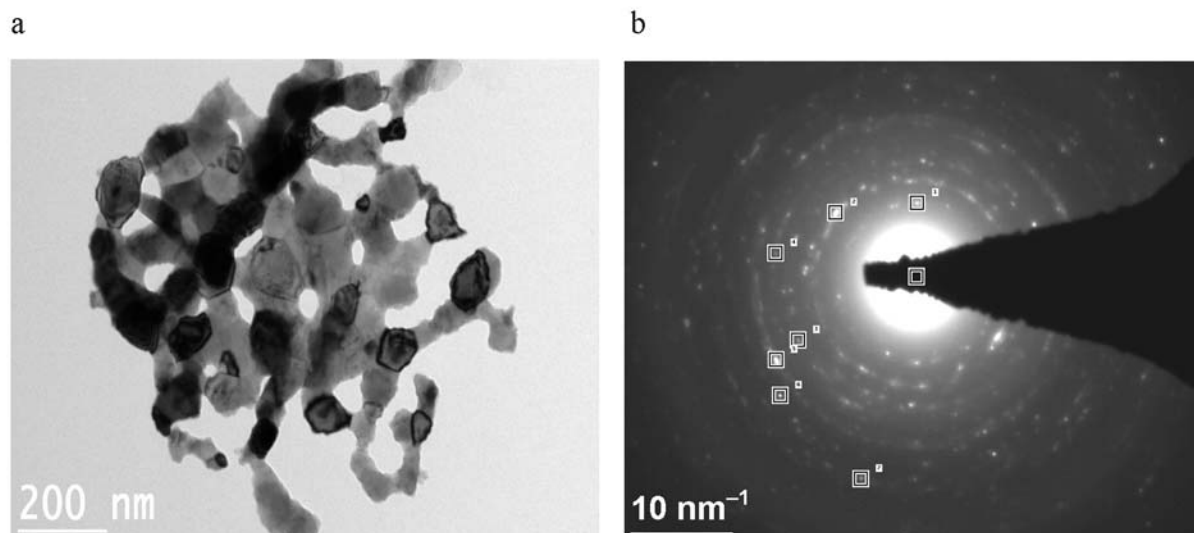


Fig. 4. TEM image of CdO nanopowder (a) and SAED pattern of CdO nanopowder (b).

Scanning electron microscopy (SEM)

Morphologies of the combustion derived CdO nanopowder and the commercial CdO powders were examined using a JEOL-JSM-6490 LV scanning electron microscope (SEM). The SEM image of commercial CdO powder (Fig. 3a) revealed that the commercial powder has very low porosity compared to that of the combustion derived CdO nanopowder. The SEM micrograph of CdO nanopowder (Fig. 3b) shows that the powder is porous and agglomerated with polycrystalline nanoparticles. The pores and voids can be attributed to the large amount of gas escaping during the combustion. The macroporous framework is composed of accessible mesochannels with a wormhole-like array. It can be seen that the macropore sizes are not as homogeneously distributed as the mesoporous ones. This is due to the non uniform distri-

bution of porous secondary particles. The observed mesoporosity can be referred to the voids between the interconnected primary particles; the macroporosity results from voids between the secondary particles. Mesopores provide large surface area and active sites, and macropores enhance mass diffusion of the reactant molecules during the catalysis (Yuan et al., 2004; Blin et al., 2003; Khaleel & Al-Mansouri, 2010).

Transmission electron microscopy (TEM)

The micrograph in Fig. 4a shows a network of large particles of moderate sizes and irregular shapes formed by agglomeration of well dispersed nanoparticles with the average size of 40–60 nm. The size of these nanoparticles is in good agreement with the values obtained from XRD experiments. In order to obtain deep insight into the pore morphology of this

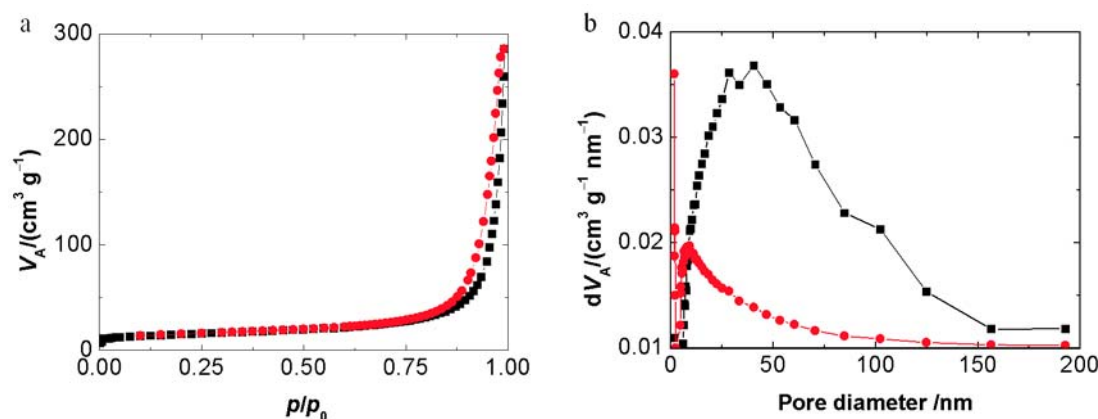


Fig. 5. Nitrogen adsorption–desorption isotherm of CdO nanopowder (a) and pore size distribution curve determined from the N_2 adsorption–desorption isotherm (b): adsorption (■) and desorption (●) data.

material, the macroporous structure image of the sample was further investigated by TEM measurements (Fig. 4a). TEM directly visualized the porous network which appeared to have a higher structural order relative to macropores in the powders obtained. The polycrystalline nature of the obtained sample was confirmed by selected area electron diffraction (SAED) performed on a Hitachi model H-600 instrument operating at 100 kV as shown in Fig. 4b.

Surface area and pore size distribution

Nitrogen adsorption measurements were carried out at 77 K using the gas sorption analyzer Quanta chrome corporation NOVA 1000. Surface area of the CdO nanopowder was calculated by the BET method. CdO nanopowder has a large surface area, $34 \text{ m}^2 \text{ g}^{-1}$, compared to that of commercial CdO ($3\text{--}4 \text{ m}^2 \text{ g}^{-1}$). Surface area of the product mainly depends on the type of the fuel used. The larger surface area is attributed to the liberation of gaseous products such as H_2O , CO_2 , and N_2 during combustion; the agglomerates disintegrate and most of the heat is carried away from the system thus hindering particle growth. This larger surface area is important for catalytic/adsorbent applications because small size of the particles maximizes the surface area exposed to the reactant, allowing thus more reactions to take place. Fig. 5a shows a representative adsorption–desorption isotherm of nitrogen obtained at the temperature of liquid nitrogen and corresponding pore size distribution for CdO nanopowder which exhibited a typical type IV isotherm according to the IUPAC classification with hysteresis reflecting the mesoporosity and continuous increase in the nitrogen uptake at higher relative pressure (p/p_0) indicating the presence of macropores. These macropores are clearly distinct from the mesopores also observed in SEM and TEM images (Yuan et al., 2004).

Pore size distributions (pore diameter, pore volume), calculated from the corresponding desorption

isotherms by the BJH method, are shown in Fig. 5b. A narrow pore size distribution with an average pore diameter of 46 nm and a pore volume of $0.039 \text{ cm}^3 \text{ g}^{-1}$ can be observed. This narrow pore size distribution of mesopores with diameters between 40 nm and 50 nm exhibits a peak maximum at 46 nm which indicates the homogeneity of the mesopores of the prepared materials. Thus, SEM and TEM observations and N_2 adsorption analysis revealed that the materials exhibit a bimodal pore size distribution and that they are in fact meso–macroporous systems.

Basic site measurement

About 0.15 g of CdO nanopowder was inserted into the centrifuge tube and 10 mL of distilled water were added. The mixture was shaken vigorously and then allowed to stand for 24 h at room temperature. The solution was centrifuged to separate the solid from the liquid phase. Supernatant liquid was transferred into a conical flask and 10 mL of 0.1 M hydrochloric acid were added. Then, 2–3 drops of the phenolphthalein indicator were dropwise added to the mixture under vigorous shaking of the flask. The solution was titrated with NaOH (0.05 M) until the color of the solution changed from colorless to pink. The change of the color indicates that the reaction had reached its endpoint (Nondek et al., 1979; Samadi et al., 2010). The back titration carried out to estimate the basic sites present on 0.15 g of the CdO nanopowder was found to be 0.92 mmol. This result was also confirmed by FTIR and XRD studies.

Proposed mechanism of basic site measurement for CdO nanopowder

The amount of basic sites present in CdO nanopowder was determined by back titration. Eq. (2) shows the proposed mechanism for the determination of the amount of basic sites. In this reaction, the prepared CdO nanopowder was allowed to stand in dis-

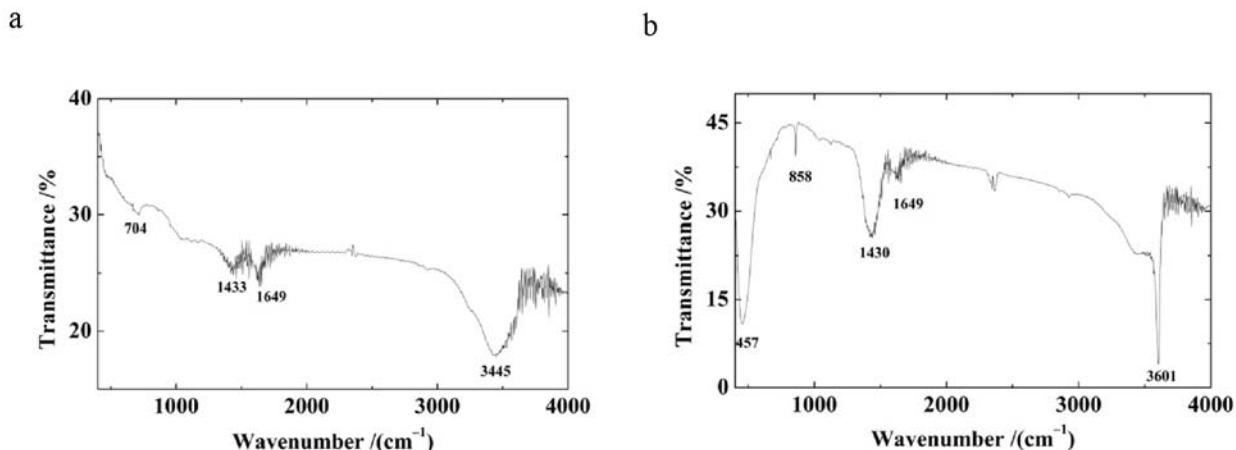


Fig. 6. FTIR spectra of CdO nanopowder (a) and H⁺ ion adsorbed on the CdO nanopowder (b).

tilled water for 24 h to let the nanoparticles of CdO submerge into distilled water. The H⁺ ion was provided by distilled water and it was absorbed by the lone pair of oxygen from the CdO nanopowder releasing the OH⁻ ion. This technique estimates the amount of the H⁺ ions absorbed by the prepared CdO nanopowder. Finally, the H⁺ ions formed a bond with the CdO nanopowder resulting in the formation of Cd(OH)₂. This mechanism was further supported by FTIR spectra (Fig. 6b) and XRD diffractogram (Fig. 2b) which confirmed the formation of Cd(OH)₂.

FTIR studies

FTIR spectrum of the CdO nanopowder is shown in Fig. 6a. The spectrum exhibits a common broad band near 3445 cm⁻¹ due to the OH-stretching vibrations of free and hydrogen-bonded hydroxyl groups, and a second typical absorption region at 1649 cm⁻¹ which is assigned to the bending vibration of water molecules, most probably caused by the water adsorption during the compaction of the powder specimens with KBr (Angappan et al., 2004). Formation of the CdO phase is characterized by poorly resolved shoulders at 704 cm⁻¹ (Ristić et al., 2004). Fig. 6b shows the FTIR spectrum of the H⁺ ion adsorbed on CdO nanopowder. The main characteristic peak is a sharp and intensive band corresponding to the OH stretching vibrations at 3601 cm⁻¹ (Angappan et al., 2004). This indicates that the adsorbed H⁺ ions are bound to the surface of the CdO nanopowder, at least partially or covalently, which resulted in the formation of Cd(OH)₂. The shoulder at 1649 cm⁻¹ can be associated with the bending vibrations of water molecules, suggesting that the CdO nanopowder contains basic sites absorbed by water molecules. IR bands in the region of 1500–1450 cm⁻¹ can be assigned to a residual organic component. In the region of lower wave numbers, IR bands at 858 cm⁻¹ and 457 cm⁻¹ which

can be assigned to Cd(OH)₂ were observed (Mazheritehrani et al., 2010).

Role of L-(+)-tartaric acid

The solution combustion reaction mainly depends on the nature of fuel, temperature, and on the stoichiometric ratio of fuel to oxidizer. In the present investigation, different organic compounds such as citric acid, malic acid, succinic acid, lactic acid, and also tartaric acid were examined as fuels in the synthesis of CdO nanopowder. Among these, tartaric acid with two OH groups and two COOH groups seems to be chemically suitable for the preparation of CdO nanopowder because of its versatile co-ordination modes and conformational flexibility (Blomqvist & Ebbe, 1984; Johnston et al., 2010; Zheng et al., 2010, 2004).

Tartaric acid plays a dual role in the synthesis of CdO nanopowder; it functions as a complexing agent, prevents the precipitation of ions by complexation with Cd²⁺ ions (Masoumeh et al., 2011), and as a fuel in the combustion reaction. During the combustion reaction, a redox reaction takes place resulting in a very high temperature and the evolution of large volumes of gases. Even though the furnace temperature was maintained at (400 ± 10) °C, the particles could have attained higher temperature during the ignition. The heat energy released is different for different fuels based on their value of heat of combustion and hence, every system is expected to form different phases based on the total heat content of the system. Here, tartaric acid forms a polynuclear complex with Cd²⁺ ions. Morphology of the particles is generally based on the nature of the fuel, polynuclear complex formation, and on the fuel to oxidizer ratio.

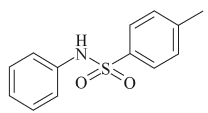
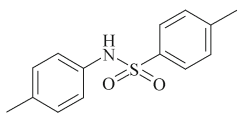
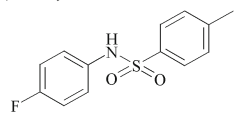
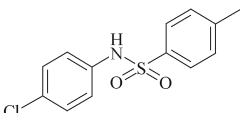
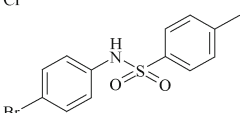
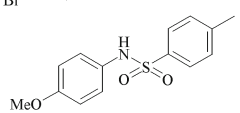
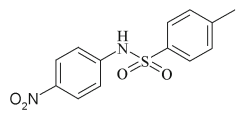
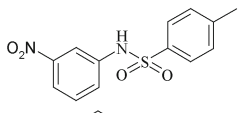
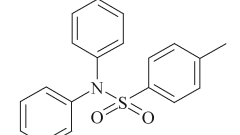
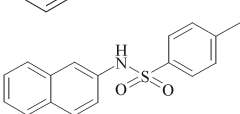
Catalytic activity

Initially, the reaction between aniline and *p*-TsCl

Table 1. Optimization of conditions for the reaction between aniline and *p*-TsCl

Entry	Catalyst	Temperature	Time	Isolated yield
		°C	min	%
1	2 mole % Commercial-CdO	25	120	40
2	3 mole % Commercial-CdO	25	120	43
3	2 mole % Commercial-CdO	Reflux	120	62
4	1 mole % Nano-CdO	25	60	75
5	1 mole % Nano-CdO	Reflux	10	95
6	–	25	120	Trace

Table 2. CdO catalyzed synthesis of sulfonamides from the reaction of amines with *p*-TsCl at reflux conditions^a

Entry	Amine	Product	Time min	Yield	
				CdO nanopowder %	Common CdO
a	Aniline		10	95	56
b	4-Toluidine		25	90	44
c	4-Fluoroaniline		15	90	45
d	4-Chloroaniline		20	92	54
e	4-Bromoaniline		25	86	42
f	4-Anisidine		15	88	49
g	4-Nitroaniline		25	89	59
h	3-Nitroaniline		30	87	43
i	Diphenylamine		30	85	42
j	2-Naphthylamine		20	90	58

a) All reactions were performed using substituted aromatic amine (5 mmol), MeCN (5 mL), *p*-TsCl (5.5 mmol), and CdO nanopowder (1 mole %), b) all compounds are known and physical properties agree with the reported values; IR and MS data match with the reported spectral data.

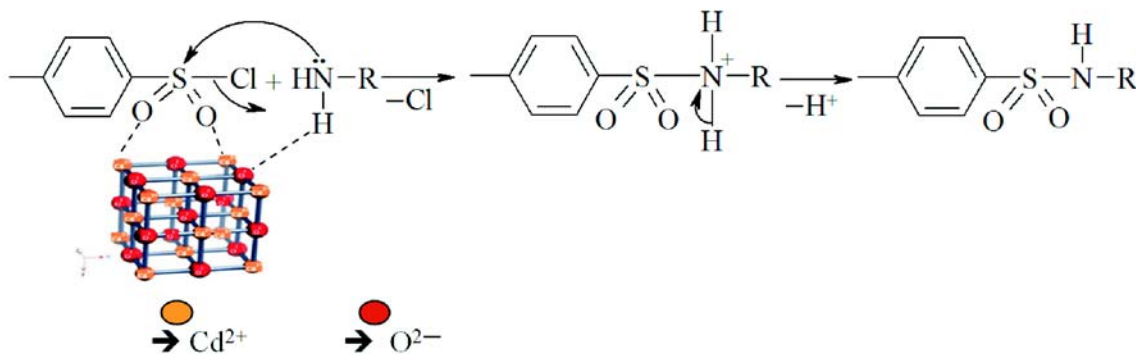


Fig. 7. Possible mechanism for catalytic activity of CdO nanopowder in sulfonation of aromatic amines with *p*-TsCl.

at room temperature was carried out using commercial CdO (2 mole %) as the catalyst in acetonitrile as a solvent and a 40 % yield of the desired product (Table 1, entry 1) was obtained. There was no significant increase in the yield of the product either with the increase of the reaction time, the temperature or the amount of CdO (Table 1, entry 2). When the same reaction was carried out using 1 mole % of CdO nanopowder, 75 % of the product (Table 1, entry 4) were obtained. The increased catalytic activity of CdO nanopowder over the commercial CdO can be attributed to the larger surface area of the CdO nanopowder (SA: $34 \text{ m}^2 \text{ g}^{-1}$) compared to that of commercial CdO (SA: $3\text{--}4 \text{ m}^2 \text{ g}^{-1}$). Catalytic activity of the CdO nanopowder was evident when a negligible amount of the product was obtained in the absence of the catalyst even after 2 hours of the reaction (Table 1, entry 6).

To reduce the reaction time and to improve the yield of the product, the reaction was carried out at reflux condition. Aromatic amines were sulfonylated using MeCN as the solvent at reflux condition and a 95 % yield was obtained within 10 min of the reaction (Table 1, entry 5). To determine the general applicability of this process, syntheses of a variety of sulfonamides were studied (Table 2). It is noteworthy that 1-naphthylamine can also be used to obtain the corresponding sulfonamide in a good yield (Table 2, entry j), which is also of interest due to its biological activity. The use of just 1 mole % of the CdO nanopowder in MeCN was found to be sufficient for the reaction to take place. Higher amounts of the CdO nanopowder did not provide higher yields. The yields are, in general, very high regardless of the structural variations in amines. The products obtained are of high purity.

It is important to note that the synthesis procedure is very simple. The catalyst was collected by filtration and the filtrate was evaporated to get the pure product.

*Possible mechanism for catalytic activity of CdO nanopowder in sulfonation of aromatic amines with *p*-toluenesulfonyl chloride*

To understand the relationship between the structure and the reactivity of the catalyst in this reaction it is important to know the structure and nature of the reactive sites of CdO nanopowder. The catalyst has a polycrystalline, three dimensional cubic structure with high surface concentrations of edges, corners, and various exposed crystal planes (111), (200), (220), (311), and (222), which leads to inherently high surface reactivity per unit area. Moreover, CdO nanopowder has Lewis acid sites Cd^{2+} , Lewis basic sites O^{2-} and O^- , lattice bound, and anionic and cationic vacancies (Fahim & Abd El-Salaam, 1967; Chintareddy & Kantam, 2011). Acid-base and redox properties are important surface chemical properties of metal oxide catalysts. Since the CdO nanopowder is found to be more basic, it is more efficient in the sulfonation reaction of amines than the commercial CdO powder.

Thus, CdO nanopowder displays higher activity compared to the commercial CdO powder. In the first step of the reaction, H of the amino group of the aromatic amine is expected to be activated by O^{2-} (Lewis base) and *p*-toluenesulfonyl group can be activated by Cd^{2+} (Lewis acid) of nanocrystalline CdO. The activated substrates can react with each other to form the corresponding product *I* as shown in Fig. 7.

Recycling studies

Experiments were conducted to determine the reusability of the catalyst. The catalyst can be easily separated by filtration and it can be reused after its activation at 200°C for one hour in a muffle furnace. Efficiency of the recovered catalyst was tested using a model reaction under similar conditions (Table 2, entry a). Using the fresh catalyst, the yield of the product (Table 2, entry a) was 95 % while the recovered catalyst in the three subsequently repeated experiments provided yields of 94 %, 90 %, and 91 %, respectively.

respectively. These results demonstrate that the catalyst can be reused several times without a significant loss of its activity.

Conclusions

A simple combustion synthesis using tartaric acid as a fuel to obtain CdO nanopowder has been developed. We are the first to develop the process of CdO nanopowder synthesis and employ it as a catalyst in the sulfonylation of amines with *p*-toluenesulfonyl chloride to rapidly obtain sulfonamides in an excellent yield (85–95 %) and high purity under mild reaction conditions. The catalyst can be recovered by simple filtration and reused in four cycles without any significant loss of its catalytic activity.

Acknowledgements. Gujjarahalli Thimmanna Chandrappa gratefully acknowledges financial support of the University Grants Commission, New Delhi, to carry out this research work. The authors are thankful to Prof. Sarala Upadhya, Department of Mechanical Engineering, UVCE, Bangalore University, for recording SEM images and to Prof. Jai Prakash, Bangalore Institute of Technology for surface area measurements.

References

- Abd El-Salaam, K. M., & Hassan, E. A. (1982). Active surface centres in a heterogeneous CdO catalyst for ethanol decomposition. *Surface Technology*, 16, 121–128. DOI: 10.1016/0376-4583(82)90031-0.
- Alves, M. B., Medeiros, F. C. M., & Suarez, P. A. Z. (2010). Cadmium compounds as catalysts for biodiesel production. *Industrial & Engineering Chemistry Research*, 49, 7176–7182. DOI: 10.1021/ie100172u.
- Anderson, K. K. (1979). Sulphonic acids and their derivatives. In D. N. Jones (Ed.), *Comprehensive organic chemistry* (Vol. 3, pp. 345). Oxford, UK: Pergamon Press.
- Angappan, S., Bechermans, L. J., & Augustin, C. O. (2004). Sintering behaviour of MgAl₂O₄—a prospective anode material. *Materials Letters*, 58, 2283–2289. DOI: 10.1016/j.matlet.2004.01.033.
- Ashoka, S., Chithaiah, P., & Chandrappa, G. T. (2010). Studies on the synthesis of CdCO₃ nanowires and porous CdO powder. *Materials Letters*, 64, 173–178. DOI: 10.1016/j.matlet.2009.10.036.
- Askarinejad, A., & Morsali, A. (2008). Syntheses and characterization of CdCO₃ and CdO nanoparticles by using sonochemical method. *Materials Letters*, 62, 478–482. DOI: 10.1016/j.matlet.2007.05.082.
- Balandin, A. A., Ferapontov, V. A., & Tolstopyatova, A. A. (1960). The activity of cadmium oxide as catalyst for hydrogen dehydrogenation. *Russian Chemical Bulletin*, 9, 1630–1636. DOI: 10.1007/bf00906559.
- Blin, J. L., Léonard, A., Yuan, Z. Y., Gigot, L., Vantomme, A., Cheetham, A. K., & Su, B. L. (2003). Hierarchically mesoporous/macroporous metal oxides templated from polyethylene oxide surfactant assemblies. *Angewandte Chemie*, 115, 2978–2981. DOI: 10.1002/ange.200250816.
- Blomqvist, K., & Ebbe, R. (1984). Solution studies of systems with polynuclear complex formation. 5. Copper(II) and cadmium(II) D-(+)-tartrate systems. *Inorganic Chemistry*, 23, 3730–3734. DOI: 10.1021/ic00191a013.
- Chan, Y. W., & Berthelette, C. (2002). A mild, efficient method for the synthesis of aromatic and aliphatic sulfonamides. *Tetrahedron Letters*, 43, 4537–4540. DOI: 10.1016/s0040-4039(02)00848-1.
- Chandrasekhar, S., & Mahapatra, S. (1998). Neighbouring group assisted sulfonamide cleavage of Sharpless aminols under acetonation conditions. *Tetrahedron Letters*, 39, 695–698. DOI: 10.1016/s0040-4039(97)10638-4.
- Chintareddy, V. R., & Kantam, M. L. (2011). Recent developments on catalytic applications of nano-crystalline magnesium oxide. *Catalysis Surveys from Asia*, 15, 89–110. DOI: 10.1007/s10563-011-9113-0.
- Davis, M. E. (2002). Ordered porous materials for emerging applications. *Nature*, 417, 813–821. DOI: 10.1038/nature00785.
- Fahim, R. B., & Abd El-Salaam, K. M. (1967). Surface properties and hydration of cadmium oxide. *Journal of Catalysis*, 9, 63–69. DOI: 10.1016/0021-9517(67)90181-9.
- Gliński, M., Kijeński, J., & Jakubowski, A. (1995). Ketones from monocarboxylic acids: Catalytic ketonization over oxide systems. *Applied Catalysis A: General*, 128, 209–217. DOI: 10.1016/0926-860x(95)00082-8.
- Harter, W. G., Albrecht, H., Brady, K., Caprathe, B., Dunbar, J., Gilmore, J., Hays, S., Kostlan, C. R., Lunney, B., & Walker, N. (2004). The design and synthesis of sulfonamides as caspase-1 inhibitors. *Bioorganic & Medicinal Chemistry Letters*, 14, 809–812. DOI: 10.1016/j.bmcl.2003.10.065.
- Johnston, L. L., Nettleman, J. H., Braverman, M. A., Sposato, L. K., Supkowski, R. M., & LaDuca, R. L. (2010). Copper benzenedicarboxylate coordination polymers incorporating a long-spanning neutral co-ligand: Effect of anion inclusion and carboxylate pendant-arm length on topology and magnetism. *Polyhedron*, 29, 303–311. DOI: 10.1016/j.poly.2009.05.022.
- Khaleel, A., & Al-Mansouri, S. (2010). Meso-macroporous γ -alumina by template-free sol-gel synthesis: The effect of the solvent and acid catalyst on the microstructure and textural properties. *Colloid Surface A: Physicochemical and Engineering Aspects*, 369, 272–280. DOI: 10.1016/j.colsurfa.2010.08.040.
- Madhusudana Reddy, M. B., Ashoka, S., Chandrappa, G. T., & Pasha, M. A. (2010). Nano-MgO: An efficient catalyst for the synthesis of formamides from amines and formic acid under MWI. *Catalysis Letters*, 138, 82–87. DOI: 10.1007/s10562-010-0372-6.
- Madhusudana Reddy, M. B., Ashoka, S., Anandakumar, B. S., Chandrappa, G. T., & Pasha, M. A. (2011). Combustion derived nanocrystalline-ZrO₂ and its catalytic activity for Biginelli condensation under microwave irradiation. *Chinese Journal of Chemistry*, 29, 1863–1868. DOI: 10.1002/cjoc.201180325.
- Masoumeh, T., Alefeh G., Elaheh, K., & Masood, P. (2011). Two tartrate-pillared coordination polymers: Hydrothermal preparation, crystal structures, spectroscopic and thermal analyses of {[M₂(μ -C₄H₄O₆)₂(H₂O)] · 3H₂O}_∞ (M = Mn, Cd). *Journal of Inorganic and Organometallic Polymers and Materials*, 21, 627–633. DOI: 10.1007/s10904-011-9495-5.
- Mazaheritehrani, M., Asghari, J., Lotfi Orimi, R., & Pahlavan, S. (2010). Microwave-assisted synthesis of nano-sized cadmium oxide as a new and highly efficient catalyst for solvent free acylation of amines and alcohols. *Asian Journal of Chemistry*, 22, 2554–2564.
- Nagappa, B., & Chandrappa, G. T. (2007). Mesoporous nanocrystalline magnesium oxide for environmental remediation. *Micropores and Mesopores Materials*, 106, 212–218. DOI: 10.1016/j.micromeso.2007.02.052.
- Nishida, H., Hamada, T., & Yonemitsu, O. (1988). Hydrolysis of tosyl esters initiated by an electron transfer from photoexcited electron-rich aromatic compounds. *Journal of Organic Chemistry*, 53, 3386–3387. DOI: 10.1021/jo00249a058.

- Nondek, L., Vít, Z., & Málek, J. (1979). Determination of basic sites on the surface of metal oxide catalysts by desorption of benzoic acid. *Reaction Kinetics and Catalysis Letters*, *10*, 7–11. DOI: 10.1007/bf02067504.
- O'Connell, J. F., & Rapoport, H. (1992). 1-Benzenesulfonyl- and 1-*p*-toluenesulfonyl-3-methylimidazolium triflates: efficient reagents for the preparation of arylsulfonamides and arylsulfonates. *The Journal of Organic Chemistry*, *57*, 4775–4777. DOI: 10.1021/jo00043a046.
- Okuhara, T., & Tanaka, K. I. (1980). Intermediates of hydrogenation of conjugated dienes and of the isomerization of *n*-butenes on CdO catalyst. *Journal of Catalysis*, *61*, 135–139. DOI: 10.1016/0021-9517(80)90348-6.
- Patil, K. C., Hegde, M. S., Rattan, T., & Aruna, S. T. (2008). *Chemistry of nanocrystalline oxide materials: Combustion synthesis, properties and applications*. Danvers, MA, USA: World Scientific.
- Poissonnet, G., Théret-Bettiol, M. H., & Dodd, R. H. (1996). Preparation and 1,3-dipolar cycloaddition reactions of β -carboline azomethine ylides: A direct entry into C-1- and/or C-2-functionalized indolizino[8,7-*b*]indole derivatives. *The Journal of Organic Chemistry*, *61*, 2273–2282. DOI: 10.1021/jo951520t.
- Reddy, N. S., Mallireddigari, M. R., Cosenza, S., Gumireddy, K., Bell, S. C., Reddy, E. P., & Reddy, M. V. R. (2004). Synthesis of new coumarin 3-(*N*-aryl) sulfonamides and their anticancer activity. *Bioorganic & Medicinal Chemistry Letters*, *14*, 4093–4097. DOI: 10.1016/j.bmcl.2004.05.016.
- Ristić, M., Popović, S., & Musić, S. (2004). Formation and properties of Cd(OH)₂ and CdO particles. *Materials Letters*, *58*, 2494–2499. DOI: 10.1016/j.matlet.2004.03.016.
- Russell, M. G. N., Baker, R. J., Barden, L., Beer, M. S., Bristow, L., Broughton, H. B., Knowles, M., McAllister, G., Patel, S., & Castro, J. L. (2001). *N*-Arylsulfonylindole derivatives as serotonin 5-HT₆ receptor ligands. *Journal of Medicinal Chemistry*, *44*, 3881–3895. DOI: 10.1021/jm010943m.
- Samadi, N. S., Amat Mustajab, M. K. A., & Yacob, A. R. (2010). Activation temperature effect on the basic strength of prepared aerogel MgO (AP-MgO). *International Journal of Basic & Applied Sciences*, *10*(2), 118–121.
- Santos-Cruz, J., Torres-Delgado, G., Castaneda-Perez, R., Zúñiga-Romero, C. I., & Zelaya-Angel, O. (2007). Optical and electrical characterization of fluorine doped cadmium oxide thin films prepared by the sol-gel method. *Thin Solid Films*, *515*, 5381–5385. DOI: 10.1016/j.tsf.2007.01.036.
- Scozzafava, A., Owa, T., Mastrolorenzo, A., & Supuran, C. T. (2003). Anticancer and antiviral sulfonamides. *Current Medicinal Chemistry*, *10*, 925–953. DOI: 10.2174/0929867033457647.
- Sousa, C., Pacchioni, G., & Illas, F. (1999). Ab initio study of the optical transitions of F centers at low-coordinated sites of the MgO surface. *Surface Science*, *429*, 217–228. DOI: 10.1016/s0039-6028(99)00380-5.
- Sterrer, M., Berger, T., Diwald, O., & Knözinger, E. (2003). Energy transfer on the MgO surface, monitored by UV-induced H₂ chemisorption. *Journal of the American Chemical Society*, *125*, 195–199. DOI: 10.1021/ja028059o.
- Stranix, B. R., Lavallée, J. F., Sévigny, G., Yelle, J., Perron, V., LeBerre, N., Herbart, D., & Wu, J. J. (2006). Lysine sulfonamides as novel HIV-protease inhibitors: *N*-Acyl aromatic α -amino acids. *Bioorganic & Medicinal Chemistry Letters*, *16*, 3459–3462. DOI: 10.1016/j.bmcl.2006.04.011.
- Supuran, C. T., Casini, A., & Scozzafava, A. (2003). Protease inhibitors of the sulfonamide type: Anticancer, antiinflammatory, and antiviral agents. *Medical Research Reviews*, *23*, 535–558. DOI: 10.1002/med.10047.
- Thakuria, H., Borah, B. M., & Das, G. (2007). Macroporous metal oxides as an efficient heterogeneous catalyst for various organic transformations—A comparative study. *Journal Molecular Catalysis A: Chemical*, *274*, 1–10. DOI: 10.1016/j.molcata.2007.04.024.
- Waghulade, R. B., Patil, P. P., & Pasricha, R. (2007). Synthesis and LPG sensing properties of nano-sized cadmium oxide. *Talanta*, *72*, 594–599. DOI: 10.1016/j.talanta.2006.11.024.
- Yasuhara, A., Kameda, M., & Sakamoto, T. (1999). Selective monodesulfonylation of *N,N*-disulfonylarylamines with tetrabutylammonium fluoride. *Chemical and Pharmaceutical Bulletin*, *47*, 809–812.
- Yuan, W., Fearson, K., & Gelb, M. H. (1989). Synthesis of sulfur-substituted phospholipid analogs as mechanistic probes of phospholipase A2 catalysis. *The Journal of Organic Chemistry*, *54*, 906–910. DOI: 10.1021/jo00265a034.
- Yuan, Z. Y., Ren, T. Z., Vantomme, A., & Su, B. L. (2004). Facile and generalized preparation of hierarchically mesoporous-macroporous binary metal oxide materials. *Chemistry of Materials*, *16*, 5096–5106. DOI: 10.1021/cm0494812.
- Zhang, G., Zhao, Z., Liu, J., Xu, J., Jing, Y., Duan, A., & Jiang, G. (2009). Macroporous perovskite-type complex oxide catalysts of La_{1-x}K_xCo_{1-y}Fe_yO₃ for diesel soot combustion. *Journal of Rare Earths*, *27*, 955–960. DOI: 10.1016/s1002-0721(08)60369-5.
- Zheng, Y. Q., Lin, J. L., & Kong, Z. P. (2004). Coordination polymers based on cobridging of rigid and flexible spacer ligands: Syntheses, crystal structures, and magnetic properties of [Mn(bpy)(H₂O)(C₄H₄O₄)]·0.5bpy, Mn(bpy)(C₅H₆O₄), and Mn(bpy)(C₆H₈O₄). *Inorganic Chemistry*, *43*, 2590–2596. DOI: 10.1021/ic0301268.
- Zheng, Y. Q., Han, X. Y., & Zhu, H. L. (2010). Syntheses, crystal structures and properties of tetrahydrofuran-2,3,4,5-tetracarboxylato bridged copper(II) coordination polymers with alkali metals. *Polyhedron*, *29*, 911–919. DOI: 10.1016/j.poly.2009.10.022.